# Phase Diagram for Spontaneous Nuclear Magnetic Ordering in Copper

M. T. Huiku, T. A. Jyrkkiö, J. M. Kyynäräinen, A. S. Oja, and O. V. Lounasmaa
*Low Temperature Laboratory, Helsinki University of Technology, SF-02150 Espoo 15, Finland*
(Received 13 June 1984)

The static susceptibility of a single-crystal copper specimen has been measured at nanokelvin temperatures, parallel and perpendicular to the external magnetic field $B$. Below $B_c = 0.27$ mT, three different antiferromagnetically ordered regions are described at small values of entropy $S$. The $B$-$S$ phase diagram is presented. Metastabilities and the observed nonadiabaticity during the final stages of demagnetization are discussed.

PACS numbers: 75.30.Kz, 75.30.Cr, 75.50.Ee

This Letter presents, for the first time, an experimentally determined phase diagram of magnetically ordered nuclear spins in a metal. Antiferromagnetism in copper nuclei is achieved after demagnetization to a small field $B$ where spin-spin interactions dominate. The static susceptibility has been measured at nanokelvin temperatures in the three Cartesian directions. In contrast to our earlier work,[1,2] the present experiments were performed on a single crystal. Nuclear ordering has been studied in some insulators at Saclay.[3]

Nuclear ordering in metallic copper was first observed in a polycrystalline sample.[1] In this experiment metastability was observed in field sweeps to 1 mT and then back to zero again, which indicated a first-order transition during demagnetization. We also observed a considerable supercooling of the paramagnetic phase. Two different antiferromagnetic states, labeled $A$ and $B$, were reported. In a more detailed series of experiments[2] in zero field and well below the transition temperature $T_c = 60$ nK, it was found that metastable states were present only when the initial entropy at 1 mT before demagnetization to zero field was higher than $S_i = 0.37R$ ln4. Otherwise an antiferromagnetic state ($A$) was always reached. Further, it was observed that the transition to the $A$ phase took place in 20 s after the end of demagnetization and that the entropy increased during this time by $\Delta S = 0.12R$ ln4. The exact meaning of the metastability and nonadiabaticity, however, remained unresolved.

The present series of experiments were again carried out in our two-stage nuclear demagnetization cryostat.[2,4] The specimen was a selectively oxidized,[1,5] high-purity, natural-copper, single crystal of dimensions $0.5 \times 5 \times 20$ mm$^3$ along the $x$, $y$, and $z$ axis, respectively; the external magnetic field was in the $z$ direction. By x-ray diffraction it was found that the cubic [100] crystal axis is 4° above the $(x,y)$ plane and 13° off the $x$ axis and that the [001] axis is about 8° off the $z$ axis.

The static susceptibility $\chi$ was measured, with low-frequency ac techniques and a SQUID (superconducting quantum interference device),[1,2] at a constant conduction-electron temperature $T_e = 50$–$100$ $\mu$K. Separate transverse and longitudinal SQUID systems were connected to two astatically wound signal coils, $(x,y)$ and $z$, respectively.[4] Three different excitation coils, along the $x$, $y$, and $z$ axis, were used; the alignment of the 10-Hz ac excitation field was selected by switches and variable resistances. The transverse and longitudinal signals could be obtained during a single run.

We have measured the susceptibility $\chi_i(t)$ ($i = x$, $y$, and $z$) as a function of time during the warmup of nuclear spins. As before, a characteristic increase of $\chi_i(t)$ was observed at the lowest entropies. The salient features of our data can be best described in terms of three quantities: $\chi_i^{\max}$, the maximum value of the susceptibility, $\Delta\chi_i = \chi_i^{\max} - \chi_i(t=0)$, the net rise in the susceptibility after demagnetization, and $\Delta t$, the warmup time needed to reach $\chi_i^{\max}$. In Fig. 1 we show these quantities, also illustrated in the inset at top left, for the transverse $(x,y)$ and longitudinal $(z)$ directions.

We observe from Fig. 1 that $\chi_{x,y}^{\max}$ remains constant in the ordered state. Above $B = 0.25$ mT, $\chi_{x,y}^{\max}$ starts to decrease as expected in the paramagnetic phase. $\Delta\chi_y$, on the other hand, shows considerable variation. It is largest, over 7%, in an external field between 0 and 0.04 mT. After a rapid drop, a low plateau can be seen around $B = 0.08$ mT. At 0.10 mT, $\Delta\chi_y$ again increases and between 0.11 and 0.16 mT it is almost as large as when $B = 0$. Above $B = 0.17$ mT, $\Delta\chi_y$ decreases gradually to zero at about 0.25 mT. This is a somewhat higher field than reported in Ref. 1 because of the lower $S_i$ obtained in these experiments. In contrast, $\Delta\chi_x$ is zero and the asymmetry ($\Delta\chi_y \neq \Delta\chi_x$) is present in the entire field range. $\Delta t$ also shows interesting behavior. On the assumption that the warmup time is a monotonic function of $B_c(S)$, $\Delta t$

 

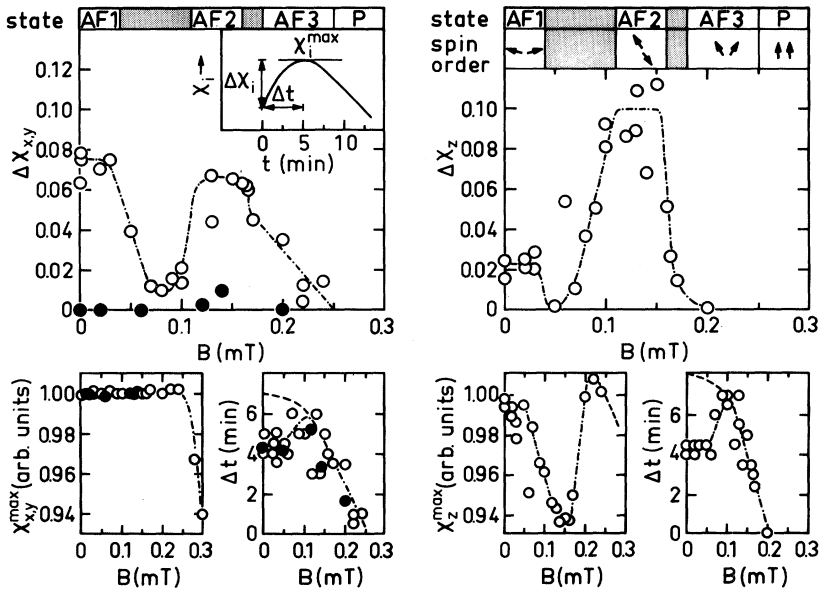


FIG. 1. The static susceptibility $\chi_i$ ($i = x, y,$ and $z$) of copper nuclear spins as a function of the external magnetic field $\vec{B} = B\hat{z}$. In the transverse geometry, shown in three figures on the left, open circles are for the $y$ direction and filled circles for the $x$ direction; data in the longitudinal ($z$) direction are shown on the right. $\Delta\chi_i$ denotes the difference of the maximum susceptibility $\chi_i^{max}$, obtained at time $\Delta t$ after the end of demagnetization, and the initial susceptibility $\chi_i$ ($t = 0$). These quantities are also defined in the inset where the time behavior of $\chi_i(t)$ is schematically illustrated. In the $x$ direction $\Delta t$ shows the length of the susceptibility plateau. The suggested spin arrangements in the various states are schematically shown above the top figure on the right; the $z$ axis points upwards. The dashed lines in the $\Delta t$ vs $B$ plots indicate the expected behavior extrapolated from the region above 0.1 mT. For all data, $S_i = 0.10R \ln 4$.

should be longer in low fields. The measurements, however, disagree with this prediction below $B = 0.1$ mT. The expected behavior, extrapolated from the region $B > 0.1$ mT, is shown by the dashed line in the $\Delta t$ vs $B$ graph.

The longitudinal susceptibility $\chi_z(t)$ in the ordered state was measured for the first time during the present series of experiments. The results are shown in Fig. 1, again in terms of $\chi_z^{max}$, $\Delta\chi_z$, and $\Delta t$. We note that $\chi_z^{max}$ is smallest at $B = 0.15$ mT; the value is about 6% less than in zero field. Just above 0.20 mT, $\chi_z^{max}$ is largest, but in still higher fields it decreases. $\Delta\chi_z$ is small in low fields. It grows to about 10% between 0.11 and 0.15 mT, after which a steep decrease follows. In contrast to $\Delta\chi_y$, $\Delta\chi_z$ vanishes already at 0.20 mT and $\chi_z(t)$ decreases always as a function of time. This is illustrated in Fig. 2, where the susceptibilities $\chi_i(t)$ are shown following demagnetization to 0.20 mT. The same behavior as in the transverse direction is seen in the longitudinal $\Delta t$ vs $B$ plot.

The present data on $\chi_y(t)$ can be compared to the transverse susceptibility measured earlier on a polycrystalline sample[1,2]: The data on both specimens are qualitatively similar. The small differences are probably caused by defects in the polycrystalline lattice and by the different value of $S_i$. Because only $\Delta\chi_y$ was measured in previous experiments the now observed ($x$,$y$) asymmetry could not be seen earlier. We assume that the cause of the asymmetry is the flat-slab shape of the sample. An essential difference is that metastable states were

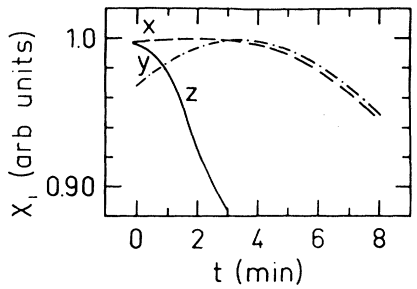


FIG. 2. The static susceptibility $\chi_i(t)$ in the three Cartesian directions $x$, $y$, and $z$ after demagnetization to 0.20 mT. The longitudinal ($z$) and transverse ($x$,$y$) susceptibilities are characteristically different between 0.18 and 0.25 mT.

not found in the present series of experiments.

Three different ordered regions can be deduced from the data seen in Figs. 1 and 2. These conclusions are obtained from a comparison between the transverse and longitudinal susceptibilities and by using the well known fact that $\chi$ perpendicular to the sublattice magnetization stays constant below $T_c$ and that $\chi$ parallel approaches zero as $T \rightarrow 0$. The first antiferromagnetic phase, AF1, where the spin vector $\vec{d}$ tends parallel to [010], is stable in the lowest fields as shown in Fig. 1. It is probable that the AF1 structure is the same as the one predicted in zero field by mean-field theory[6] with use of the combined dipolar and Ruderman-Kittel interactions of the experimentally measured strengths.[4] A wide first-order transition region separates AF1 from AF2. This second antiferromagnetic phase, between $B = 0.11$ and 0.16 mT, has a large component of $\vec{d}$ in the $z$ direction and a smaller component in the $y$ direction. The transition between AF1 and AF2 (previously reported as $A \rightarrow B$) was suggested to be of the spin-flop type.[1] We now regard it improbable, since the susceptibility data indicate a change in the antiferromagnetic spin arrangement rather than a spin-flop transition.

A third antiferromagnetic phase, AF3, can be identified between $B = 0.18$–$0.25$ mT. The characteristics of this phase are a decreasing $\chi_z(t)$ with time and an increasing $\chi_y(t)$, i.e., antiferromagnetism in the longitudinal direction has vanished (see Fig. 2). The spins are leaning towards $\vec{B} = B\hat{z}$ and, therefore, this state has a magnetic moment in the $z$ direction and a small staggered magnetization parallel to $y$. According to susceptibility data, the AF2 and AF3 phases have different symmetry operations and thus the transition between them is of first order. The change to the paramagnetic phase proceeds by tilting the spins more and more towards $\vec{B}$ until AF3 and $P$ are the same.

The thermodynamics of demagnetized copper nuclear spins can best be characterized by a state with variables $S$ and $B$. The nuclei are thermally isolated from all external heat reservoirs on time scales shorter than the spin-lattice relaxation time $\tau_1 \simeq 1$ h. The system, however, is mechanically coupled to the external world by the magnetic field. Therefore, the assembly of spins can be described by the magnetic enthalpy $H(S,B)$, rather than by the Gibbs free energy $G(T,B)$ used for systems in contact with a heat bath.

The $B$-$S$ phase diagram of copper was measured by changing the initial entropy $S_i/R$ ln4 between 0.10 and 0.50 before final demagnetization from 1 mT to lower fields. $S_i$ (equal to $S$ above $B = 0.1$ mT) was determined by varying the demagnetization procedure: We waited at 1 mT for different lengths of time. The entropy increase during and before waiting was carefully calculated with the experimental spin-lattice relaxation rate. By measurement of $\chi_y(t)$ and $\chi_z(t)$ and by use of the known characteristics of the ordered states, phase boundaries could be determined. The results are shown in Fig. 3. A shadowed region indicates that a first-order phase change is proceeding in this area. During the transition, neighboring phases coexist as macroscopic domains. The critical field at $S = 0$ is extrapolated to $B_c = 0.27$ mT.

The relation between entropy and temperature[2] ($T = dQ/dS$) could not be determined in the present experiments because, as a result of eddy current shielding in the high-conductivity single-crystal specimen, we were not able to measure the absorptive component $\chi''$ of the dynamic susceptibility ($dQ \propto \chi''$). Deviations from the expected behavior of the $\Delta t$ vs $B$ plots arise from the entropy increase during demagnetization below $B = 0.1$ mT. The gain $\Delta S = 0.12R$ ln4 in zero field was estimated with the relaxation rate of the dipolar energy in the paramagnetic state during a 3-min period. This $\Delta S$ is the same as that observed in the earlier experiments.[2]

The reason for the 12% nonadiabaticity during demagnetization is supercooling. When, during a rapid change of magnetic field, a first-order phase boundary is reached, either the AF3 or the $P$ phase

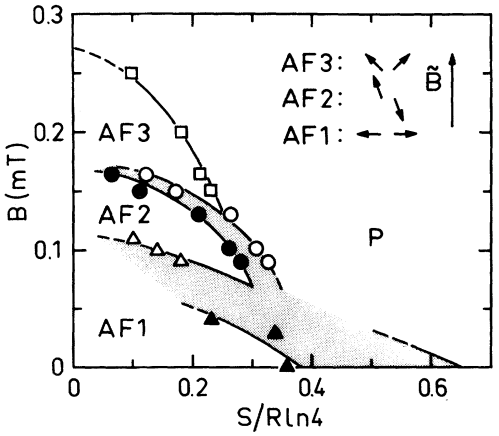


FIG. 3. The external field vs entropy diagram for nuclear ordering in copper. Different symbols denote measured data points along the respective phase boundaries. Shadowed areas indicate regions in which first-order transitions take place. The end of the first-order phase boundary in zero field at $S = 0.65R$ ln4 was determined from our earlier data on a polycrystalline sample (Ref. 2).

supercools. This is due to the long nucleation time of the AF1 and AF2 phases, probably caused by macroscopic domain-wall motion in the coexistence region. The supercooled state relaxes after demagnetization in a constant field towards equilibrium by increasing its entropy. In the AF1 phase, $\Delta S$ corresponds to the measured entropy gain of $0.12R$ ln4; in AF2, $\Delta S$ is much smaller and it could not be seen in our experiments. The entropy for the measured points below 0.05 mT in Fig. 3 was obtained by adding $\Delta S$ to $S_i$.

The existence of metastable states in the polycrystalline sample investigated earlier can also be explained by supercooling: The time scale during which the nonequilibrium state reaches equilibrium is different in a single crystal from that in a polycrystal. The relaxation towards pure AF1 takes place quickly, in about 20 s, as reported in Ref. 2. Above $S=0.37R$ ln4, the equilibrium state consists of domains of the AF1 and $P$ phases. Because of slow domain-wall motion and the large susceptibility of the supercooled paramagnetic phase, our earlier experiments showed a large, slowly relaxing $\chi^T$. In a polycrystal, grain boundaries and other defects slow down domain-wall motion. In a single crystal, the time scale is shorter and metastable states are difficult to observe.

To conclude, we have measured the $B$-$S$ phase diagram for nuclear ordering in metallic copper. Three different antiferromagnetic phases have been found. Long nucleation times, caused by domain-wall motion in the first-order phase transition regions, lead to supercooling, which explains the observed nonadiabatic demagnetization and the existence of metastable states. However, the present experiments cannot give detailed information on the nuclear magnetic structures, which must be verified by neutron-diffraction techniques. Such experiments are planned for the future.

We are indebted to J. Kurkijärvi, M. T. Loponen, M. M. Salomaa, and, in particular, to P. Kumar for useful discussions. M.H. wishes to thank the Emil Aaltonen Foundation for a scholarship. This work was supported by the Academy of Finland.

[1]M. T. Huiku and M. T. Loponen, Phys. Rev. Lett. **49**, 1288 (1982).

[2]M. T. Huiku, T. A. Jyrkkiö, M. T. Loponen, and O. V. Lounasmaa, in *Quantum Fluids and Solids—1983,* edited by E. D. Adams and G. G. Ihas, AIP Conference Proceedings No. 103 (American Institute of Physics, New York, 1983), p. 441. See also M. T. Huiku, T. A. Jyrkkiö, and M. T. Loponen, Phys. Rev. Lett. **50**, 1516 (1983).

[3]A. Abragam and M. Goldman, *Nuclear Magnetism: Order and Disorder* (Clarendon, Oxford, 1982), Chap. 8.

[4]G. J. Ehnholm, J. P. Ekström, J. F. Jacquinot, M. T. Loponen, O. V. Lounasmaa, and J. K. Soini, J. Low Temp. Phys. **39**, 417 (1980).

[5]M. T. Huiku, M. T. Loponen, T. A. Jyrkkiö, J. M. Kyynäräinen, A. S. Oja, and J. K. Soini, in *Proceedings of the Seventeenth International Conference on Low Temperature Physics,* edited by U. Eckern, A. Schmid, W. Weber, and H. Wühl (North-Holland, Amsterdam, 1984), p. 133.

[6]L. H. Kjäldman and J. Kurkijärvi, Phys. Lett. **71A**, 454 (1979).